Atmospheric Forcing of Sea Surface Temperature Decadal Variability in the Subtropical Northeastern Pacific

Yu Zhang[1,2], Shi-Yun Yu[1,3*], Dillon J. Amaya[4,5], Yu Kosaka[6], Malte F. Stuecker[7], Jun-Chao Yang[1,2], Kai-Yuan Li[3], Lei Fan[1,3], and Xiaopei Lin[1,2*]

[1] Frontiers Science Center for Deep Ocean Multispheres and Earth System and Physical Oceanography Laboratory, Ocean University of China, Qingdao, China

[2] Qingdao National Laboratory for Marine Science and Technology, Qingdao, China

[3] College of Oceanic and Atmospheric Sciences, Ocean University of China, Qingdao, China

[4] Cooperative Institute for Research in Environmental Sciences, University of Colorado Boulder, Boulder, Colorado

[5] Department of Atmospheric and Oceanic Sciences, University of Colorado Boulder, Boulder, Colorado

[6] Research Center for Advanced Science and Technology, The University of Tokyo, Tokyo, Japan

[7] Department of Oceanography and International Pacific Research Center, School of Ocean and Earth Science and Technology, University of Hawaiʻi at Mānoa, Honolulu, Hawaiʻi

Corresponding author: Shi-Yun Yu (yushiyun1177@stu.ouc.edu.cn), Xiaopei Lin (linxiaop@ouc.edu.cn)

Key Points:

- SST anomalies in the subtropical northeastern Pacific (SNEP) exhibit pronounced decadal variability.
- Both tropical Pacific-forced and internal atmospheric variability drive the SNEP SST decadal variability.
- Tropical Pacific-forced Aleutian low variability contributes to forcing the SNEP SST decadal variabilit.

Abstract

The subtropical northeastern Pacific (SNEP) acts as a bridge conveying information between the North and tropical Pacific. While most studies have investigated the SNEP sea surface temperature (SST) interannual variability, less attention has been paid to the pronounced decadal variability in this region. Here, by analyzing observational data and an ensemble pacemaker simulation, we investigate SNEP SST decadal variability in terms of atmospheric forcing processes. We find that both tropical Pacific-forced and internal (independent of tropical Pacific forcing) atmospheric variability play important forcing roles. In particular, tropical Pacific-excited Aleutian low variability, whose center of action shifts southeastward compared to the climatology, contributes to forcing SNEP SST decadal variability. This contribtution could offer an important source for the predictability of SNEP SST decadal variability.

Plain Language Summary

The subtropical northeastern Pacific is a key region of interaction between climate in the low and high latitudes of the Pacific. Sea surface temperatures (SST) in this region vary on both short (interannual) and long (decadal) timescales, of which the latter is less investigated in the literature. Our study shows that SST decadal variability in this region is effectively driven by North Pacific atmospheric conditions. These conditions can be either caused by remote tropical Pacific SST anomalies or generated independent of tropical Pacific influence. Specifically, tropical Pacific-excited Aleutian low variability can extend from its center in the mid-latitudes to the subtropics, thereby contributing to the forcing of SST decadal variability therein. This tropical Pacific-forced Aleutian low variability might help with skillful predictions of decadal climate variability in the region.

1 Introduction

The subtropical northeastern Pacific (SNEP hereafter) is a key region that affects the predictability of tropical Pacific climate variability (Amaya, 2019; Amaya et al., 2019; Chiang & Vimont, 2004; Di Lorenzo et al., 2015; Larson & Kirtman, 2014; Ma et al., 2017; Stuecker, 2018; Vimont et al., 2003), which further extends its reach globally via the atmospheric bridge (Alexander et al., 2002). Previous studies mostly focused on the SNEP sea surface temperature (SST) variability on interannual timescales. For example, the Pacific Meridional Mode (PMM; Amaya, 2019; Chiang & Vimont, 2004), whose northern node is situated in the SNEP, has been suggested to be dominantly forced by the North Pacific Oscillation (NPO; Walker & Bliss, 1932), the second empirical mode of sea level pressure (SLP) variability over the North Pacific. In addition, PMM variability in the SNEP is also influenced remotely by SST variability in the tropical North Atlantic (Ham et al., 2013; Ma et al., 2021; Wang et al., 2017), which in turn is largely driven by the El Niño–Southern Oscillation (ENSO; Amaya & Foltz, 2014; Zhang et al. 2021). Specifically, SST anomalies in the tropical North Atlantic can induce an atmospheric Gill-type response (Gill, 1980), resulting in SLP anomalies near the SNEP, which subsequently induce SNEP SST anomalies mainly through the wind-evaporation-SST feedback (Xie & Philander, 1994). In addition, studies have shown that SNEP SST variability can be affected by large-scale marine heatwaves initiated in the northeast Pacific (Amaya et al., 2020; Di Lorenzo & Mantua, 2016). For instance, the unprecedented 2014-15 marine heatwave, dubbed the Blob, was generated in the Gulf of Alaska at the start of 2014, propagated along the west coast of North America, and then impacted SST in the SNEP in winter 2014/15 (Di Lorenzo & Mantua, 2016).

While the SST interannual variability in the SNEP is well documented, there is less focus on its decadal variability. Recent studies noted that the PMM also exhibits prominent decadal variability (Liu et al., 2019; Stuecker, 2018; Zhang et al., 2021). For example, Zhang et al. (2021) investigated PMM decadal variability without equatorial Pacific influence based on a mechanically decoupled experiment in which climatological wind stress was imposed over the tropical Pacific. By this design, the experiment effectively removes interannual ENSO and equatorial Pacific decadal variability (EPDV), both of which strongly rely on dynamical ocean-atmosphere coupling (Liu & Di Lorenzo, 2018; Timmermann et al., 2018). They found that PMM decadal variability is primarily forced by atmospheric variability without equatorial Pacific influence, including the NPO and a North Pacific tripole (NPT) pattern, which is the fourth leading mode of SLP variability over the North Pacific. In contrast, with tropical Pacific influence, Stuecker (2018) highlighted the important role of tropical Pacific-forced Aleutian low (AL) variability in driving PMM decadal variability. These contrasting views on the relative contributions between tropical Pacific-forced and internal atmospheric variability to driving PMM decadal variability need to be synthesized.

In the present study, we will investigate SST decadal variability in the SNEP region (150°W-110°W, 10°N-30°N; solid box in Fig. 1a), onto which different empirical modes of SST variability in the North Pacific project (Fig. 2a-c). We will show that both tropical Pacific-forced and internal atmospheric variability contribute to forcing SNEP SST decadal variability. Internal variability in this study refers to the variability unforced by tropical Pacific SST variations. Further, we will show that the contribution from tropical Pacific-forced atmospheric variability is mainly attributed to the tropical Pacific-forced AL variability, whose center of action shifts southeastward compared to its climatology, thereby affecting the strength of northeasterly trade winds and forcing SNEP SST decadal variability. The contribution from the tropical Pacific-forced AL variability could offer an important source for the predictability of SNEP SST decadal variability.

2 Data and methods

We investigated the SNEP SST decadal variability based on observations. We used monthly SST data from the Hadley Centre Global Sea Ice and Sea Surface Temperature version 1.1 (HadISSTv1.1; Rayner et al., 2003). We also used atmospheric reanalysis data of monthly SLP and 10-m wind from the NOAA-CIRES-DOE Twentieth Century Reanalysis version 3 (20CRv3; Slivinski et al., 2019). Both data have 1° by 1° horizontal resolution. For investigating SNEP SST decadal variability, we used long time period from 1900 to 2015. We analyzed the anomaly of all variables obtained by removing the monthly climatology and linear trend. Conclusions drawn in this study will not change if based on the ECMWF Twentieth Century Reanalysis (Poli et al., 2016) and the NOAA Extended Reconstructed SST version 5 (Huang et al., 2017) from 1900 to 2010 (not shown).

To investigate the roles of tropical Pacific-forced and internal atmospheric variability in forcing SNEP SST decadal variability, we used a tropical Pacific pacemaker experiment (Pacific Ocean-Global Atmosphere, POGA; Kosaka & Xie, 2013, 2016; Yang et al., 2020; Zhang et al., 2018) based on the Geophysical Fluid Dynamics Laboratory Coupled Model version 2.1 (CM2.1; Delworth et al., 2006). The POGA simulation consists of 10 ensemble members; each member was forced by identical observed SST anomalies in the tropical eastern Pacific (from 180° to the American coast, 15°S-15°N, with a 5° buffer zone north, south, and west of the domain) as well as CMIP5 historical and representative concentration pathway 4.5 (RCP4.5) radiative forcing from 1861 to 2014, but with slightly different atmosphere-ocean initial conditions. To remove the effect of radiative forcing, we used a 20-member ensemble of CM2.1 historical simulations, each forced by historical and RCP4.5 radiative forcing and different initial conditions. The tropical Pacific-forced component is obtained by subtracting the ensemble mean of the historical experiments from the ensemble mean of the POGA experiments; internal variability is estimated by subtracting the ensemble mean of the POGA experiments from each POGA member. We analyzed the two components from 1900 to 2014. For more details on the POGA framework see Kosaka and Xie (2016).

A SNEP index is defined as the normalized monthly SST anomalies averaged over the SNEP region. To test whether SNEP SST decadal variability is primarily forced by atmospheric variability, we construct a first-order autoregressive model (AR-1) following Di Lorenzo and Mantua (2016):

$$\frac{dSST(t)}{dt} = \alpha SLP(t) - \frac{SST(t)}{\tau}, \qquad (1)$$

where $SST(t)$ is the normalized reconstructed monthly SNEP index; $SLP(t)$ is a normalized monthly principal component (PC) of SLP defined later; dt is the time step of 1 month; α is a scaling factor associated with the forcing term, which is 1 mon^{-1}; τ is the *e*-folding timescale of 9 months, estimated from the decorrelation timescale of the SNEP index (autocorrelation drops to 1/*e*; Fig. S1). Slightly changing the value of τ does not affect the conclusions drawn in this study. We then correlate decadal variability of the reconstructed SST index with the decadal SNEP index. Decadal variability in this study refers to the 10-yr low-pass Lanczos filtered variability.

The significance test for the correlation analysis is based on the two-tailed Student's *t*-test. The effective sample size is the length of the decadal SNEP index divided by its *e*-folding decorrelation timescale. The effective degree of freedom is thus the effective sample size minus 2, which is 28 for our data. Therefore, the correlation coefficient is statistically significant at the 95% confidence level if its absolute value exceeds 0.36.

3 Results

We first show that SST anomalies in the SNEP region exhibit pronounced decadal variability. Figure 1a shows the standard deviation pattern of observed SST decadal variability in the North Pacific. SST decadal variability in the SNEP is marked (averaged standard deviation is 0.22°C), with anomalies comparable to that in the western-central North Pacific (dashed box in Fig. 1a; averaged standard deviation is 0.28°C) where strong decadal variability of the Kuroshio-Oyashio extension (KOE) exists (Kwon et al., 2010). The SNEP index also exhibits marked decadal variability, with notable decadal transition in the late 1970s and late 1990s (Fig. 1b).

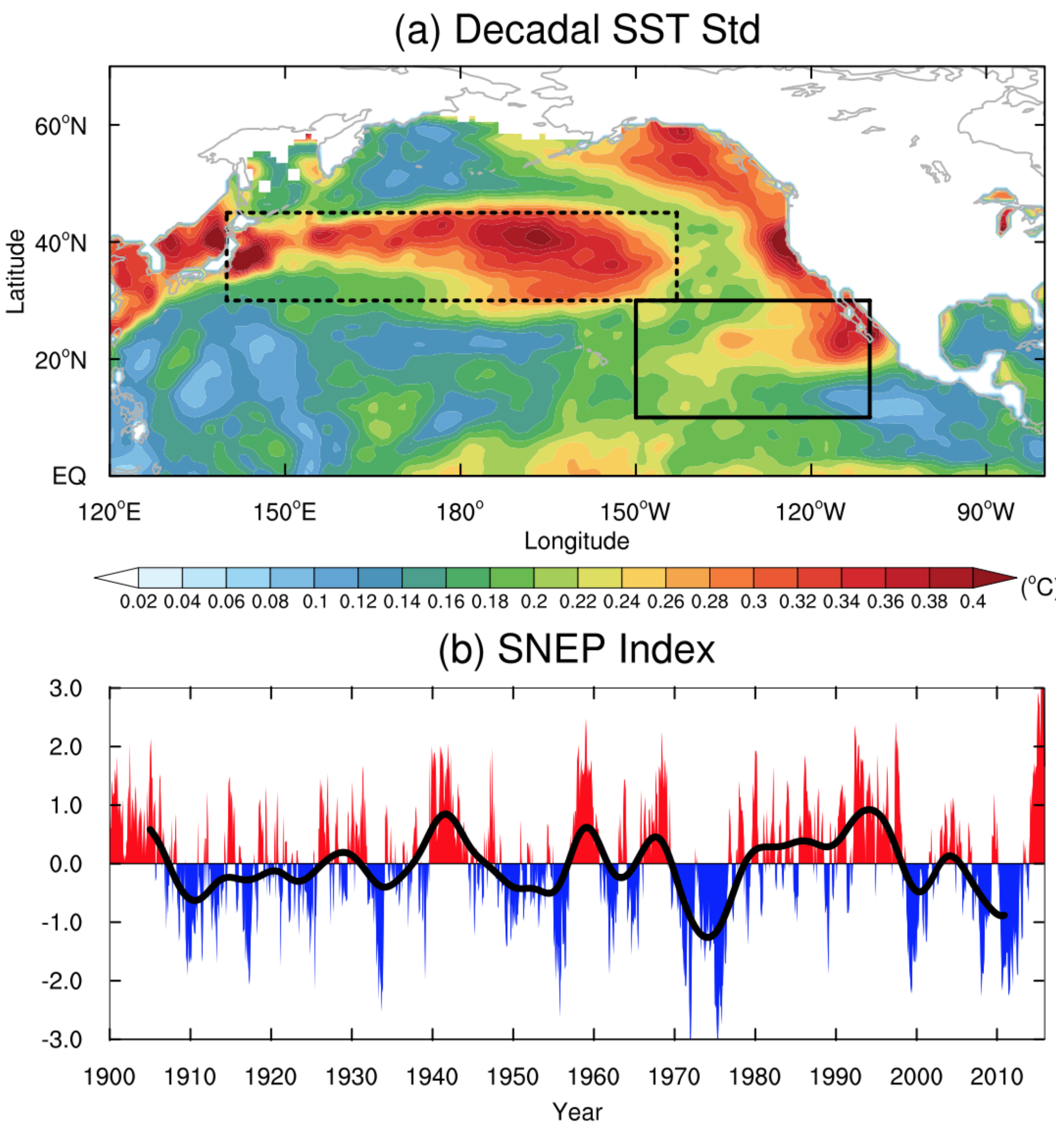

Figure 1. **Standard deviation pattern of decadal North Pacific SST variability and the SNEP index in observations.** (a) Standard deviation of decadal SST anomalies (°C) in the North Pacific. Solid box denotes the SNEP region, and dashed box denotes the western-central North Pacific region. (b) Red and blue bars denote the normalized monthly SNEP index, and the black line denotes the decadal SNEP index.

We further explore the relationship between SNEP SST decadal variability and decadal variability of leading empirical modes of North Pacific SST anomalies, which include the PMM, the Pacific Decadal Oscillation (Mantua et al., 1997), and the Victoria Mode (Bond et al., 2003). The PMM is extracted by performing a singular value decomposition (SVD) analysis between monthly SST and 10-m wind anomalies over the tropical Pacific (21°S-32°N, 175°E-95°W) after linearly removing the cold tongue index (CTI), the same procedure as Chiang and Vimont (2004). The PDO and VM are extracted by performing an empirical orthogonal function (EOF) analysis of monthly SST anomalies poleward of 20°N. The spatial patterns of the leading modes are obtained by regressing monthly SST anomalies against SST expansion coefficient (for the PMM) and normalized PCs (for the PDO and VM), respectively (Fig. 2a-c). Their decadal temporal evolutions are the 10-yr low-pass filtered SST expansion coefficient and normalized PCs, respectively (purple lines in Fig. 2d-f).

The result shows that, interestingly, SNEP SST decadal variability is strongly related to the decadal evolution of PMM variability (Fig. 2d), suggesting that the decadal SNEP index can be a good indicator of PMM decadal variability. Moreover, SNEP SST decadal variability is highly correlated with the PDO decadal variability (Fig. 2e). Since the PDO is suggested to be mainly forced by AL variability (Newman et al., 2016; Zhang et al., 2018), the high correlation implies that SNEP SST decadal variability may be partly contributed by AL forcing. We will explore this in more detail in the later sections. Finally, SNEP SST decadal variability is moderately correlated with the VM decadal variability (Fig. 2f), as seen in the moderate imprint of the VM-related SST anomalies in the SNEP region (Fig. 2c).

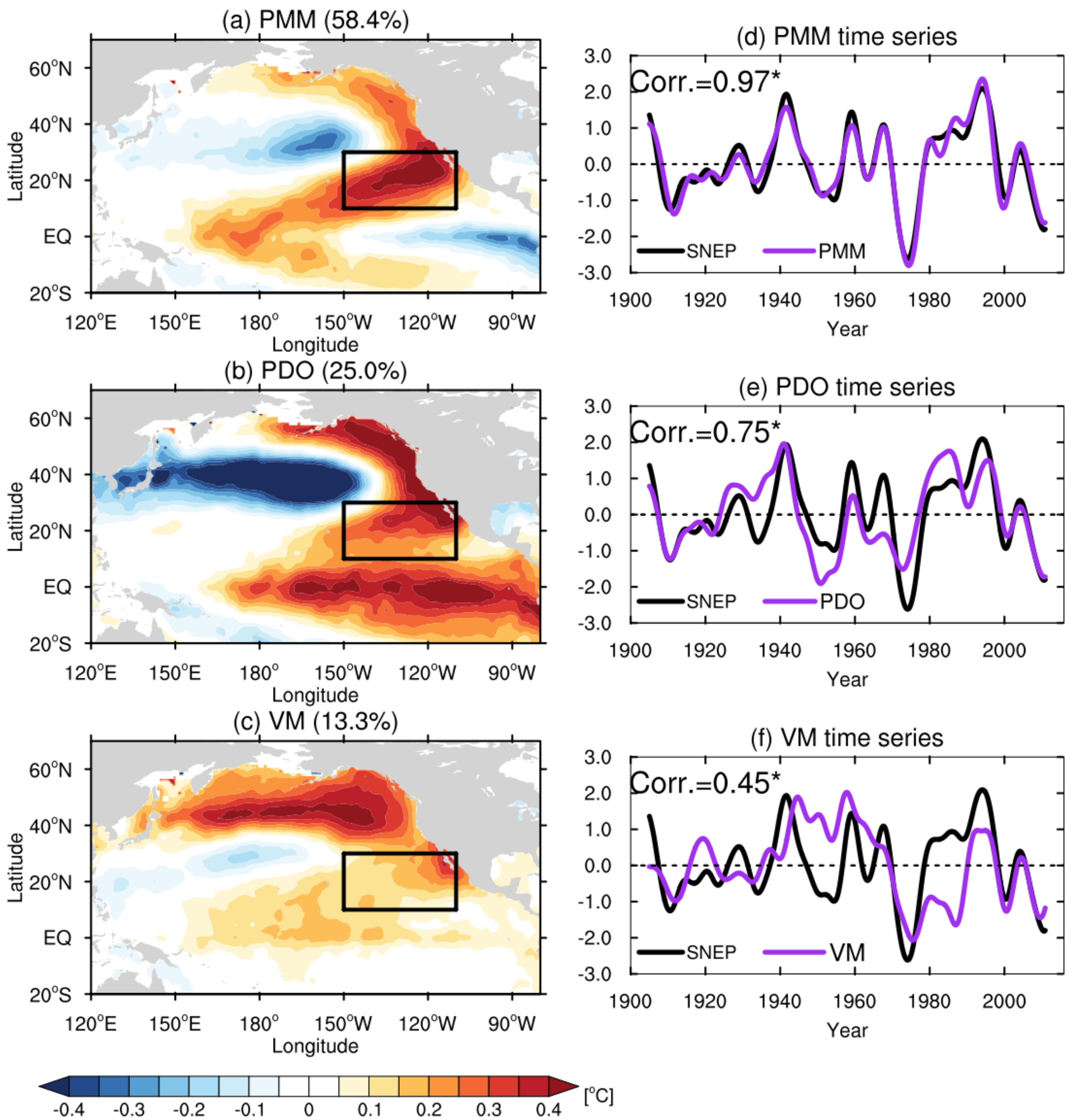

Figure 2. **Leading empirical modes of North Pacific SST variability and associated decadal time series in observations.** (a)-(c) Patterns (°C) of the PMM, PDO, and VM, respectively. The squared covariance fraction for the PMM and the explained variance for the PDO and VM are marked in each title. Black boxes denote the SNEP region. (d)-(f) Purple lines denote the 10-yr

low-pass filtered SST expansion coefficient (for the PMM) and normalized PCs (for the PDO and VM), respectively. Black lines denote the decadal SNEP index. Correlation coefficients between the PMM, PDO, VM decadal time series and the decadal SNEP index are marked in each panel, respectively, with an asterisk denoting statistical significance at the 95% confidence level.

Now we investigate which dominant modes of atmospheric variability over the North Pacific notably contribute to forcing SNEP SST decadal variability. We perform an EOF analysis of monthly SLP anomalies over the North Pacific (10°N-80°N, 130°E-110°W), and then regress monthly SLP, 10-m wind, and SST anomalies against the normalized PC of each SLP mode. Each normalized PC is used for reconstructing an SST index based on the AR-1 model (equation 1), and each 10-yr low-pass filtered reconstructed SST index is compared to the decadal SNEP index.

We will first demonstrate that North Pacific atmospheric internal variability contributes to forcing SNEP SST decadal variability. The first EOF mode of North Pacific SLP anomalies exhibits AL variability (Fig. 3a), which significantly contributes to forcing SNEP SST decadal variability (Fig. 3b). This contribution results from the AL-related surface wind anomalies over the northwest SNEP region, which relax northeasterly trade winds and thus force SST therein. Additionally, AL variability is associated with SST variations in the tropical eastern Pacific, implying that it may be the tropical Pacific-forced variability that contributes to forcing SNEP SST decadal variability. In the following, we will further explore the speculation by comparing tropical Pacific-forced and internal AL variability based on the POGA experiment. The second SLP EOF mode depicts NPO variability (Fig. 3c). It partly contributes to the forcing of SNEP

SST decadal variability as wind fluctuations associated with its southern lobe can influence the trade winds speed in the SNEP region and thereby impact SST (Fig. 3c,d). Further, NPO variability is less associated with tropical Pacific SST variations, suggesting that internal variability of the NPO plays the forcing role. This argument can be further demonstrated by the POGA simulation, in which tropical Pacific-forced NPO variability fails to drive SNEP SST decadal variability as it is somewhat weak and northeast-southwest oriented, far away from the SNEP region (Fig. S4a,b), the feature similar to the one driven by central Pacific SST anomalies (Stuecker, 2018). The third SLP EOF mode hardly contributes to forcing SNEP SST decadal variability since the pattern is located over mid-high latitudes, too far away from the SNEP (Fig. 3e,f). Finally, the fourth SLP EOF mode is NPT variability (Zhang et al, 2021). It also contributes to the forcing of SNEP SST decadal variability as wind anomalies associated with the southeastern lobe of the NPT can effectively influence the trade winds speed and therefore force the SNEP SST (Fig. 3g,h). Additionally, NPT variability moderately links tropical eastern Pacific SST variations, implying that it may be partly driven by tropical Pacific forcing. Indeed, tropical Pacific SST variability can force a weak NPT-like pattern, emerged as the fourth EOF mode of North Pacific SLP variability in the POGA ensemble mean (Fig. S2c). However, this NPT-like variability cannot effectively affect the trade winds because its southeastern lobe is displaced westward compared to the observed NPT, and thus impact the SNEP SST (Fig. S2d). These above analyses suggest that internal variability of the NPT plays the role in forcing SNEP SST decadal variability.

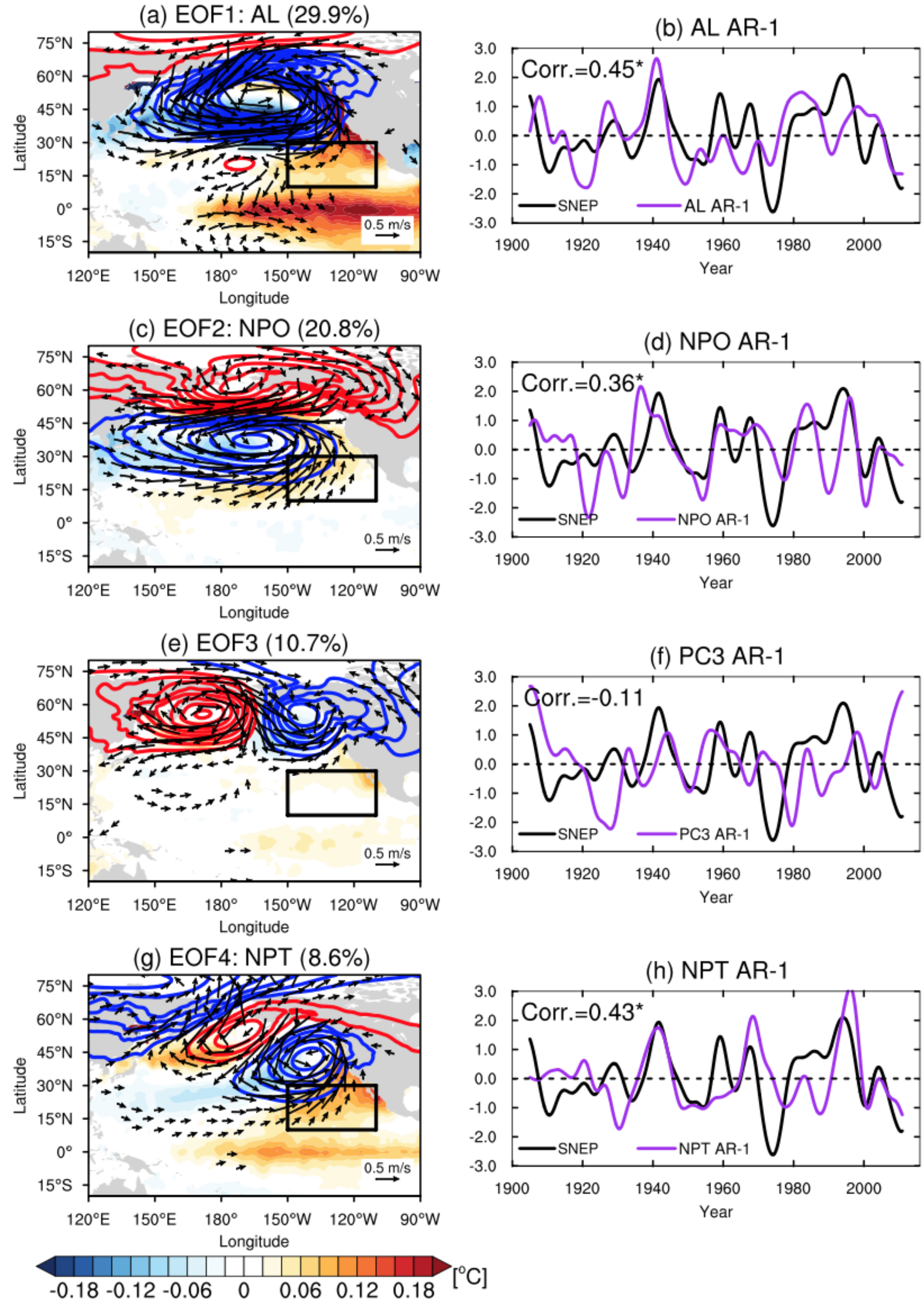

(a) EOF1: AL (29.9%)
(b) AL AR-1
Corr.=0.45*
SNEP
AL AR-1
(c) EOF2: NPO (20.8%)
(d) NPO AR-1
Corr.=0.36*
NPO AR-1
(e) EOF3 (10.7%)
(f) PC3 AR-1
Corr.=-0.11
PC3 AR-1
(g) EOF4: NPT (8.6%)
(h) NPT AR-1
Corr.=0.43*
NPT AR-1
Latitude
Longitude
Year
0.5 m/s
[°C]

235

Figure 3. Leading modes of the observed North Pacific SLP variability and their reconstructed SST indices. (a),(c),(e),(g) Regression maps of monthly SLP (contour interval: 0.4 hPa; red contours denote positive anomalies and blue contours denote negative anomalies), 10-m wind (vectors; m s^{-1}), and SST (shading; °C) anomalies against the normalized PCs of the (a) AL, (c) NPO, (e) EOF3, and (g) NPT, respectively. Regressed 10-m wind and SST anomalies are shown only significant at the 95% confidence level based on the two-tailed Student's *t*-test. The explained variance of each SLP mode is marked in each title. (b),(d),(f),(h) Decadal variability of the reconstructed SST indices (purple lines) forced by each normalized monthly SLP PC based on the AR-1 model. Black lines denote the decadal SNEP index. Correlation coefficients between the decadal reconstructed SST indices and the decadal SNEP index are marked in each panel, with an asterisk denoting statistical significance at the 95% confidence level.

Finally, we will demonstrate that AL variability driven by tropical Pacific SST anomalies also contributes to the forcing of SNEP SST decadal variability. To deomonstrate this, we use the POGA experiment to isolate the tropical Pacific-forced and internal components of AL variability by performing an EOF analysis of the monthly SLP anomalies over the North Pacific (10°N-80°N, 130°E-110°W, the same domain as used for the observations) for POGA ensemble mean and intermember spread, respectively. We then regress monthly SLP and 10-m winds anomalies against the corresponding normalized PC1s. Meanwhile, we overlay the climatological December-February AL pattern (shading in Fig. 4a,b) to compare it with the tropical Pacific-forced and internal ALs, respectively.

The result shows that compared to the climatological AL, tropical Pacific-forced AL variability shifts southeastward (Fig. 4a). As a result, it can affect the trade winds north of ~20°N and thus contribute to the forcing of SNEP SST decadal variability. The southeastward-shifted tropically forced AL variability results from the southeastward displaced center of action over the Aleutians associated with the tropical Pacific-excited Pacific-North American (PNA) pattern (Fig. S3a; Horel & Wallace, 1981), which has been documented in a number of previous studies (Stuecker, 2018; Zhang et al., 2018). In contrast, internal AL variability associated with the internally generated PNA teleconnection (Fig. S3b; Simmons et al., 1983) is located northeastward compared to the climatological AL (Fig. 4b). Therefore, it cannot effectively influence the trade winds (Fig. 4c) and force the SNEP SST, which is demonstrated by the insignificant correlations between the decadal reconstructed SST indices forced by each internal AL PC1 and the decadal SNEP indices from each POGA member (Fig. 4d). We also tested the robustness of the results based on a 20-member Community Earth System Model (CESM) POGA experiment (Deser et al., 2017; radiatively forced variability was removed by subtracting the ensemble mean of 40-member CESM historical simulations from each CESM POGA member). The results from CESM POGA are basically identical to those from CM2.1 POGA, although the southward and northward shifts of the two AL variabilities are not as strong as those in the CM2.1 POGA (Fig. S4).

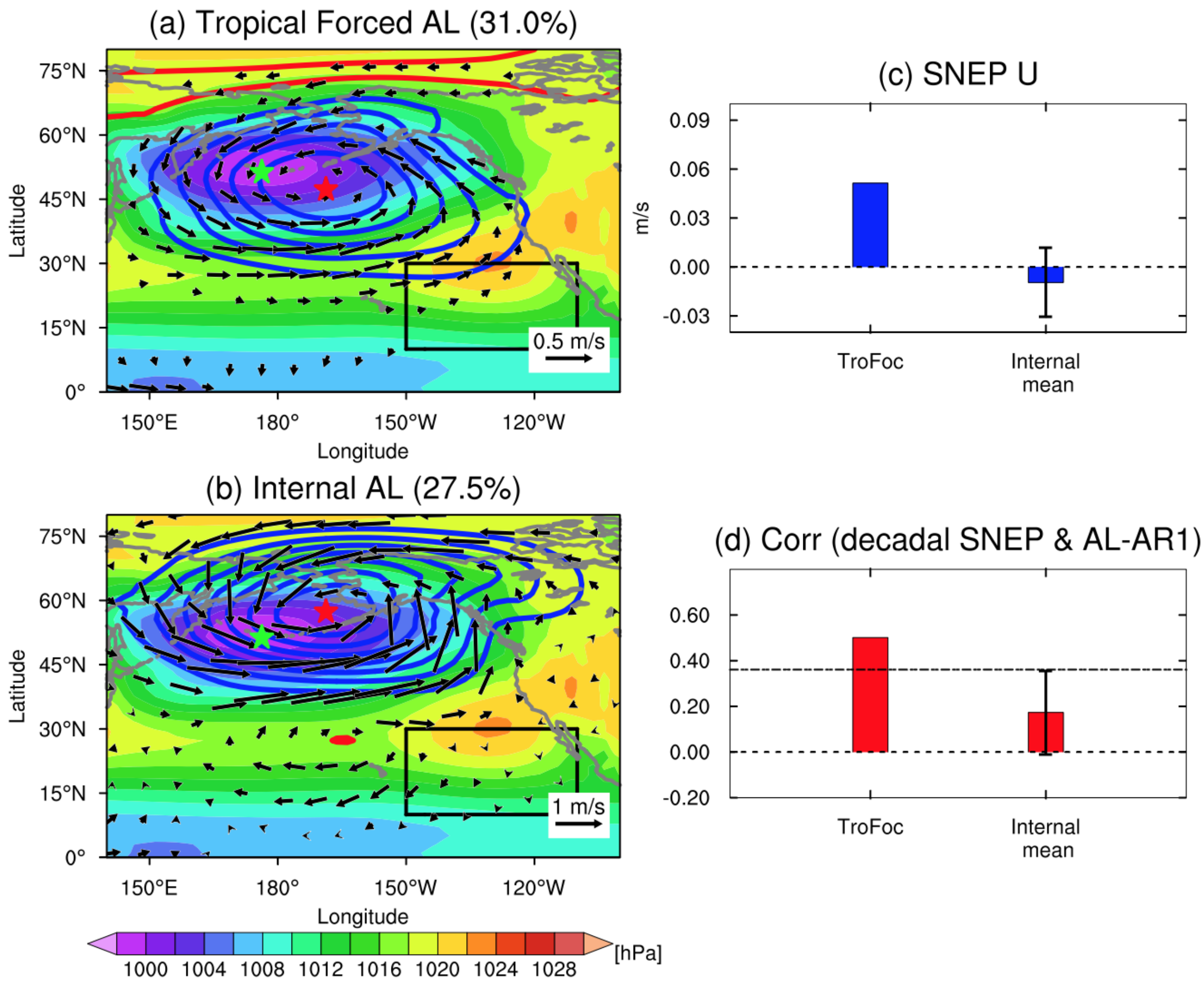

Figure 4. Tropical Pacific-forced and internal AL variability in the CM2.1 POGA experiment. (a),(b) As in Fig. 3a, but for tropical Pacific-forced (contour interval: 0.2hPa) and internal AL variability (contour internal: 0.8hPa) in the CM2.1 POGA, with red stars representing the centers of action of the two AL variabilities, respectively. The explained variances of the two AL variabilities in the CM2.1 POGA ensemble mean and intermember spread are marked in each title, respectively. Climatological SLP averaged over December-February is superimposed as shading in each panel, with green star representing the center of action of the climatological AL. Black boxes denote the SNEP region. (c) Regressed zonal wind anomalies (m s^{-1}) against the normalized monthly PC1 of tropical Pacific-forced and internal AL

variability, averaged over the SNEP region. Errorbar denotes one standard deviation of 10 regressed internal zonal wind anomalies averaged over the SNEP region. (d) TroFoc: correlation between the decadal reconstructed SST index forced by the normalized PC of tropical Pacific-forced AL variability and the decadal SNEP index. Internal mean: correlations between the decadal reconstructed SST indices forced by each normalized PC of internal AL variability and the decadal SNEP indices obtained from each CM2.1 POGA member. Red bar (errorbar) denotes the mean (one standard deviation) of the 10 correlation coefficients. Dashed line denotes the correlation coefficient significant at the 95% confidence level, which is 0.36.

4 Summary and Discussion

We have shown that SST anomalies averaged over the SNEP region, referred to as the SNEP index in this study, exhibit pronounced decadal variability. Decadal variability of the SNEP index can well track decadal evolution of PMM variability. Further, we have investigated North Pacific atmospheric forcing of SNEP SST decadal variability, suggesting that both atmospheric internal NPO and NPT and tropical Pacific-forced AL variability play important roles. Atmospheric internal AL variability, in contrast, ineffectively impact SNEP SST decadal variability because of its further northeastward displaced center of action. The forcing of tropical Pacific-excited AL variability could offer an important source for the predictability of SNEP SST decadal variability.

Although it is well known that AL variability can be generated by both tropical Pacific forcing and atmospheric internal variability (Newman et al., 2016; Zhang et al., 2018), the distinction in their longitudinal position is paid less attention, which may have some potential consequences. First, although it is known that AL variability can affect ocean dynamics in the KOE region, such as via excited westward-propagating oceanic Rossby waves (Newman et al., 2016), the different latitudinal position between the two AL variabilities may impact KOE dynamics distinctly. Second, while both of the two AL variabilities can force a PDO-like SST pattern (Newman et al., 2016; Zhang et al., 2018), their different imprints on the SNEP SST imply distinct influences on EPDV. Specifically, the PDO driven by tropical Pacific-forced AL variability can impact EPDV via the SNEP through the “fast” equatorward-propagating WES feedback (Stuecker, 2018). In contrast, the PDO driven by internal AL variability may not efficiently affect EPDV as it is located a bit far away from the subtropics. We call for more research on investigating the effects of the two AL variabilities on EPDV and other AL-related climate variability.

Acknowledgments

The HadISSTv1.1 data is available at https://www.metoffice.gov.uk/hadobs/hadisst/. The NOAA Extended Reconstructed SST version 5 data is available at https://psl.noaa.gov/data/gridded/. The 20CRv3 data is available at https://psl.noaa.gov/data/gridded/data.20thC_ReanV3.html#detail. The ECMWF Twentieth Century Reanalysis data is available at https://apps.ecmwf.int/datasets/data/era20c-moda/levtype=sfc/type=an/. The 20-member CESM POGA and 40-member CESM historical simulations are available at https://www.earthsystemgrid.org/dataset/ucar.cgd.ccsm4.output.html. The ensemble mean data of 20-member CM2.1 historical simulations are available at https://drive.google.com/drive/folders/1alZ8t4mlUCDGLtLgchpUFADW3Xv2d9TV?usp=sharing. The 10-member CM2.1 POGA data are available at https://drive.google.com/drive/folders/1fTXHcmzcFK4EmsBq28MGSAgRTq4PafL3?usp=sharing. Y.Z. and X.L. were supported by the National Natural Science Foundation of China (92058203290 and 41925025). D.J.A. was supported by a Postdoctroal Fellowship at the Cooperative Institute for Research in Environmental Sciences (CIRES) at the University of Colorado Boulder. Y.K. was supported by Japan Society for the Promotion of Science (Grants-in-Aid for Scientific Research JP18H01278 and JP19H05703) and by Japan Ministry of Education, Culture, Sports, Science and Technology (JPMXD0717935457). M.F.S. was supported by NOAA’s Climate Program Office’s Modeling, Analysis, Predictions, and Projections (MAPP) program grant NA20OAR4310445. This is IPRC publication X and SOEST contribution Y. J.-C.Y. was supported by the project funded by China Postdoctoral Science

Foundation (2020M672138) and the Fundamental Research Funds for the Central Universities (202013029). L.F. was supported by the Natural Science Foundation of China (41975089).

References

Alexander, M. A., Bladé, I., Newman, M., Lanzante, J., Lau, N.-C. & Scott, J. D. (2002). The atmospheric bridge: The influence of ENSO teleconnections on air–sea interaction over the global oceans. *Journal of Climate, 15,* 2205–2231. https://doi.org/10.1175/ 1520-0442(2002)015,2205:TABTIO.2.0.CO;2

Amaya, D. J. (2019). The Pacific Meridional Mode and ENSO: A review. *Current Climate Change Reports*, *5*, 296–307. https://doi.org/10.1007/s40641-019-00142-x

Amaya, D. J., & Foltz, G. R. (2014). Impacts of canonical and Modoki El Niño on tropical Atlantic SST. *Journal of Geophysical Research: Oceans, 119(2),* 777-789. https://doi.org/10.1002/2013JC009476

Amaya, D. J., Kosaka, Y., Zhou, W., Zhang, Y., Xie, S.-P. & Miller, A. J. (2019). The North Pacific pacemaker effect on historical ENSO and its mechanisms. *Journal of Climate*, *32*, 7643–7661. https://doi.org/10.1175/JCLI-D-19-0040.1

Amaya, D. J., Miller, A. J., Xie, S.-P., & Kosaka, Y. (2020). Physical drivers of the summer 2019 North Pacific marine heatwave. *Nature communications, 11(1),* 1-9. https://doi.org/10.1038/s41467-020-15820-w

Bond, N. A., Overland, J. E., Spillane, M., & Stabeno, P. (2003). Recent shifts in the state of the North Pacific. *Geophysical Research Letters, 30(23),* 2183. https://doi.org/10.1029/2003GL018597

Chiang, J., & Vimont, D. J. (2004). Analogous Pacific and Atlantic meridional modes of tropical atmosphere–ocean variability. *Journal of Climate*, *17*, 4143–4158. https://doi.org/10.1175/JCLI4953.1

Delworth, T. L., Broccoli, A. J., Rosati, A., Stouffer, R. J., Balaji, V., Beesley, J. A., et al. (2006). GFDL's CM2 global coupled climate models. Part I: Formulation and simulation characteristics. *Journal of Climate*, *13*, 643–674. https://doi.org/10.1175/JCLI3629.1

Deser, C., Guo, R., & Lehner, F. (2017). The relative contributions of tropical Pacific sea surface temperatures and atmospheric internal variability to the recent global warming hiatus. *Geophysical Research Letters, 44*, 7945–7954. https://doi.org/10.1002/ 2017GL074273

Di Lorenzo, E., Liguori, G., Schneider, N., Furtado, J. C., Anderson, B. T. & Alexander, M. A. (2015). ENSO and meridional modes: A null hypothesis for Pacific climate variability. *Geophysical Research Letters*, *42*, 9440-9448. https://doi.org/10.1002/2015GL066281

Di Lorenzo, E., & Mantua, N. (2016). Multi-year persistence of the 2014/15 North Pacific marine heatwave. *Nature Climate Change*, *6(11)*, 1042-1047. https://doi.org/10.1038/nclimate3082

Gill, A. E. (1980). Some simple solutions for heat-induced tropical circulation. *Quarterly Journal of the Royal Meteorological Society*, *106(449)*, 447-462. https://doi.org/10.1002/qj.49710644905

Ham, Y. G., Kug, J. S., Park, J. Y., & Jin, F. F. (2013). Sea surface temperature in the north tropical Atlantic as a trigger for El Niño/Southern Oscillation events. *Nature Geoscience, 6(2)*, 112-116. https://doi.org/10.1038/ngeo1686

Horel, J., & Wallace, J. (1981). Planetary-scale atmospheric phenom- ena associated with the Southern Oscillation. *Monthly Weather Review*, *109*, 813–829. https://doi.org/10.1175/1520-0493(1981)109,0813: PSAPAW.2.0.CO;2

Huang, B., Thorne, P. W., Banzon, V. F., Boyer, T., Chepurin, G., Lawrimore, J. H., et al. (2017). Extended reconstructed sea surface temperature, version 5 (ERSSTv5): upgrades, validations, and intercomparisons. *Journal of Climate, 30(20)*, 8179-8205. https://doi.org/10.1175/JCLI-D-16-0836.1

Kosaka, Y., & Xie, S.-P. (2013). Recent global-warming hiatus tied to equatorial Pacific surface cooling. *Nature, 501*, 403–407. https://doi.org/10.1038/nature12534

Kosaka, Y., & Xie, S.-P. (2016). The tropical Pacific as a key pacemaker of the variable rates of global warming. *Nature Geoscience, 9*, 669–673. https://doi.org/10.1038/ngeo2770

Kwon, Y. O., Alexander, M. A., Bond, N. A., Frankignoul, C., Nakamura, H., Qiu, B., & Thompson, L. A. (2010). Role of the Gulf Stream and Kuroshio–Oyashio systems in large-scale atmosphere–ocean interaction: A review. *Journal of Climate, 23(12)*, 3249-3281. https://doi.org/10.1175/2010JCLI3343.1

Larson, S. M., & Kirtman, B. P. (2014). The Pacific meridional mode as an ENSO precursor and predictor in the North American multimodel ensemble. *Journal of Climate*, *27,* 7018–7032. https://doi.org/10.1175/JCLI-D-14-00055.1

Liu, C., Zhang, W., Stuecker, M. F., & Jin, F. F. (2019). Pacific Meridional Mode-Western North Pacific tropical cyclone linkage explained by tropical Pacific quasi-decadal variability. *Geophysical Research Letters, 46(22)*, 13346-13354. https://doi.org/10.1029/2019GL085340

Liu, Z., & Di Lorenzo, E. (2018). Mechanisms and predictability of Pacific decadal variability. *Current Climate Change Reports, 4,* 128–144. https://doi.org/10.1007/s40641-018-0090-5

Ma, J., Xie, S.-P. & Xu, H. (2017). Contributions of the North Pacific meridional mode to ensemble spread of ENSO prediction. *Journal of Climate*, *30*, 9167–9181. https://doi.org/10.1175/JCLI-D-17-0182.1

Ma, J., Xie, S.-P., Xu, H., Zhao, J. & Zhang, L. (2021). Cross-basin interactions between the tropical Atlantic and Pacific in the ENSEMBLES hindcasts. *Journal of Climate*, *34,* 2459-2472. https://doi.org/10.1175/JCLI-D-20-0140.1

Mantua, N. J., Hare, S. R., Zhang, Y., Wallace, J. M. & Francis, R. C. (1997). A Pacific interdecadal climate oscillation with impacts on salmon production. *Bulletin of the American Meteorological Society, 78,* 1069–1079. https:// doi.org/10.1175/1520-0477(1997)078,1069:APICOW.2.0.CO;2

Newman, M., Alexander, M. A., Ault, T. R., Cobb, K. M., Deser, C., Di Lorenzo, E., et al. (2016). The Pacific decadal oscillation, revisited. *Journal of Climate*, *29*, 4399–4427. https://doi.org/10.1175/ JCLI-D-15-0508.1

Poli, P., Hersbach, H., Dee, D. P., Berrisford, P., Simmons, A. J., Vitart, F., et al. (2016). ERA-20C: an atmospheric reanalysis of the twentieth century. *Journal of Climate*, *29*, 4083–4097. https://doi.org/10.1175/JCLI-D-15-0556.1

Rayner, N. A., Parker, D. E., Horton, E. B., Folland, C. K., Alexander, L. V., Rowell, D. P., Kent, E. C. & Kaplan, A. (2003). Global analyses of sea surface temperature, sea ice, and night marine air temperature since the late nineteenth century. *Journal of Geophysical Research: Atmospheres, 108*, 4407. https://doi.org/10.1029/2002JD002670

Simmons, A. J., Wallace, J. M. & Branstator, G. (1983). Barotropic wave propagation and instability, and atmospheric telecon- nection patterns. *Journal of the Atmospheric Sciences, 40*, 1363–1392. https://doi.org/10.1175/1520-0469(1983)040,1363:BWPAIA.2.0.CO;2

Slivinski, L. C., Compo, G. P., Whitaker, J. S., Sardeshmukh, P. D., Giese, B. S., McColl, C., et al. (2019). Towards a more reliable historical reanalysis: Improvements for version 3 of the Twentieth Century Reanalysis system. *Quarterly Journal of the Royal Meteorological Society*, *145(724)*, 2876-2908. https://doi.org/10.1002/qj.3598

Stuecker, M. F. (2018). Revisiting the Pacific meridional mode. *Scientific Reports*, *8,* 3216. https://doi.org/10.1038/s41598-018-21537-0

Timmermann, A., An, S. I., Kug, J. S., Jin, F. F., Cai, W., Capotondi, A., et al. (2018). El Niño–Southern Oscillation complexity. *Nature*, *559*, 535–545. https://doi.org/10.1038/s41586-018-0252-6

Vimont, D. J., Wallace, J. M. & Battisti, D. S. (2003). The seasonal footprinting mechanism in the Pacific: Implications for ENSO. *Journal of Climate 16*, 2668–2675. https://doi.org/10.1175/1520-0442(2003)016<2668:TSFMIT>2.0.CO;2

Walker, G. T., & Bliss, E. W. (1932). World Weather V. *Memoirs of the Royal Meteorological Society*, *4*, 53–84.

Wang, L., Yu, J. Y., & Paek, H. (2017). Enhanced biennial variability in the Pacific due to Atlantic capacitor effect. *Nature Communications, 8(1)*, 1-7. https://doi.org/10.1038/ncomms14887

Xie, S.-P., & Philander, S. G. H. (1994). A coupled ocean-atmosphere model of relevance to the ITCZ in the eastern Pacific. *Tellus*, *46A*, 340–350. https://doi.org/10.3402/tellusa.v46i4.15484

Yang, J. C., Lin, X., Xie, S.-P., Zhang, Y., Kosaka, Y., & Li, Z. (2020). Synchronized tropical Pacific and extratropical variability during the past three decades. *Nature Climate Change, 10(5),* 422-427. https://doi.org/10.1038/s41558-020-0753-9

Zhang, W., Jiang, F., Stuecker, M. F., Jin, F. F., & Timmermann, A. (2021). Spurious North Tropical Atlantic precursors to El Niño. *Nature communications, 12(1)*, 1-8. https://doi.org/10.1038/s41467-021-23411-6

Zhang, Y., Xie, S.-P., Kosaka, Y., & Yang, J. C. (2018). Pacific decadal oscillation: Tropical Pacific forcing versus internal variability. *Journal of Climate, 31(20),* 8265-8279. https://doi.org/10.1175/JCLI-D-18-0164.1

Zhang, Y., Yu, S., Amaya, D. J., Kosaka, Y., Larson, S. M., Wang, X.,et al. (2021). Pacific Meridional Modes without Equatorial Pacific Influence. *Journal of Climate*, *34,* 5285–5301. https://doi.org/10.1175/JCLI-D-20-0573.1

Figure 1.

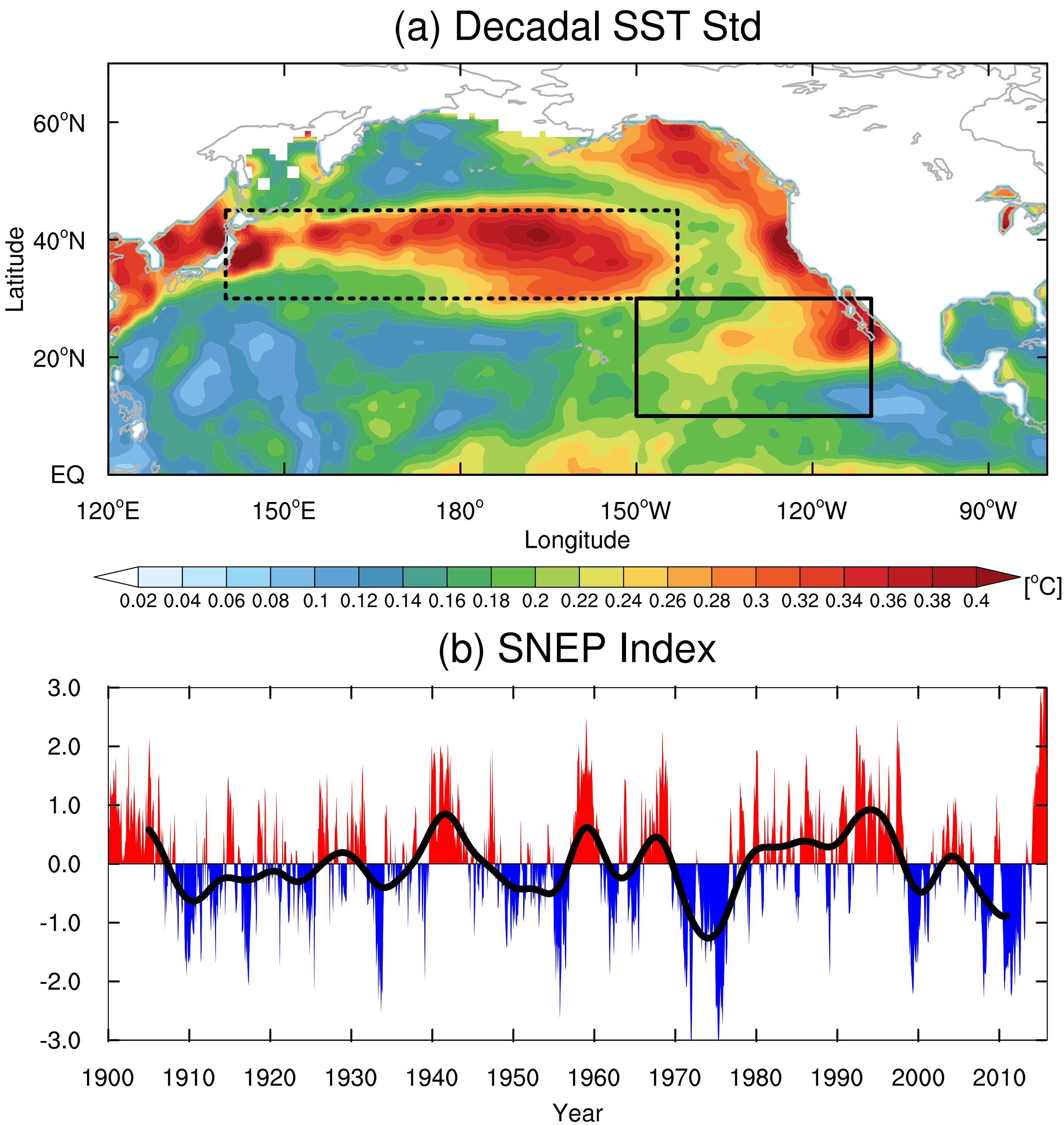

(a) Decadal SST Std
60°N
40°N
20°N
EQ
Latitude
120°E
150°E
180°
150°W
120°W
90°W
Longitude
0.02 0.04 0.06 0.08 0.1 0.12 0.14 0.16 0.18 0.2 0.22 0.24 0.26 0.28 0.3 0.32 0.34 0.36 0.38 0.4
[°C]
(b) SNEP Index
3.0
2.0
1.0
0.0
-1.0
-2.0
-3.0
1900 1910 1920 1930 1940 1950 1960 1970 1980 1990 2000 2010
Year

Figure 2.

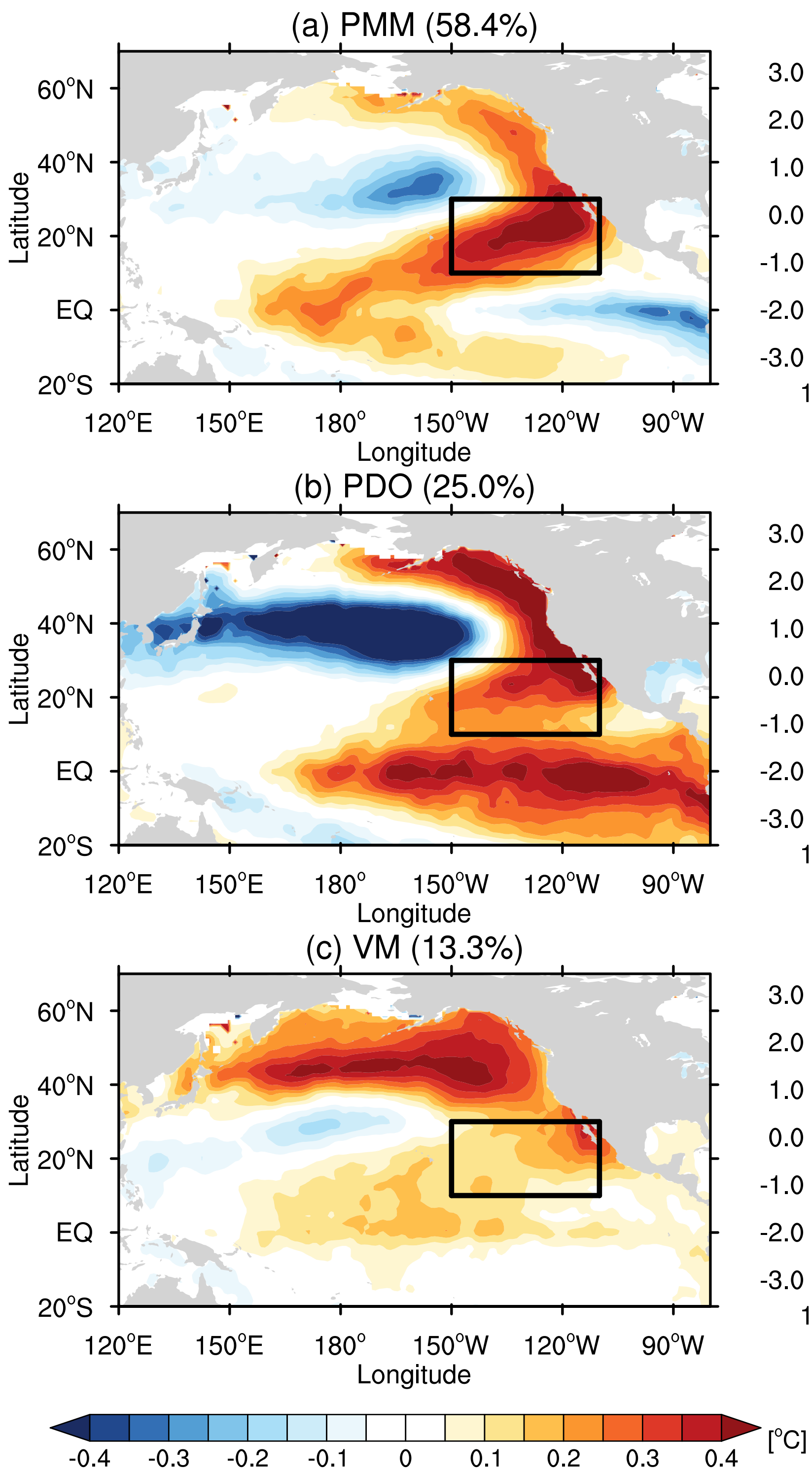

(a) PMM (58.4%)
(b) PDO (25.0%)
(c) VM (13.3%)
Latitude
Longitude
60°N
40°N
20°N
EQ
20°S
120°E
150°E
180°
150°W
120°W
90°W
(d) PMM time series
Corr.=0.97*
SNEP
PMM
(e) PDO time series
Corr.=0.75*
PDO
(f) VM time series
Corr.=0.45*
VM
Year
1900
1920
1940
1960
1980
2000
3.0
2.0
1.0
0.0
-1.0
-2.0
-3.0
-0.4
-0.3
-0.2
-0.1
0
0.1
0.2
0.3
0.4
[°C]

Figure 3.

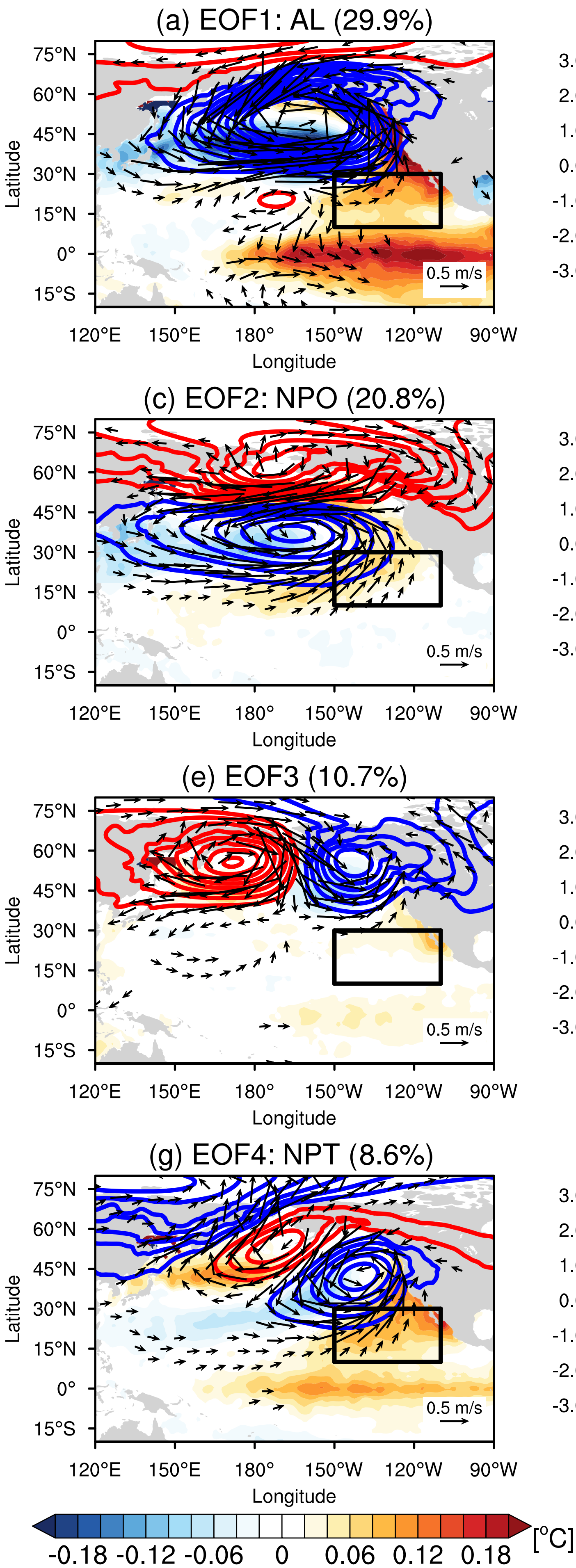

(a) EOF1: AL (29.9%)
(b) AL AR-1
Corr.=0.45*
SNEP
AL AR-1
(c) EOF2: NPO (20.8%)
(d) NPO AR-1
Corr.=0.36*
NPO AR-1
(e) EOF3 (10.7%)
(f) PC3 AR-1
Corr.=-0.11
PC3 AR-1
(g) EOF4: NPT (8.6%)
(h) NPT AR-1
Corr.=0.43*
NPT AR-1
0.5 m/s
Latitude
Longitude
Year
75°N
60°N
45°N
30°N
15°N
0°
15°S
120°E
150°E
180°
150°W
120°W
90°W
1900
1920
1940
1960
1980
2000
3.0
2.0
1.0
0.0
-1.0
-2.0
-3.0
-0.18 -0.12 -0.06 0 0.06 0.12 0.18
[°C]

Figure 4.

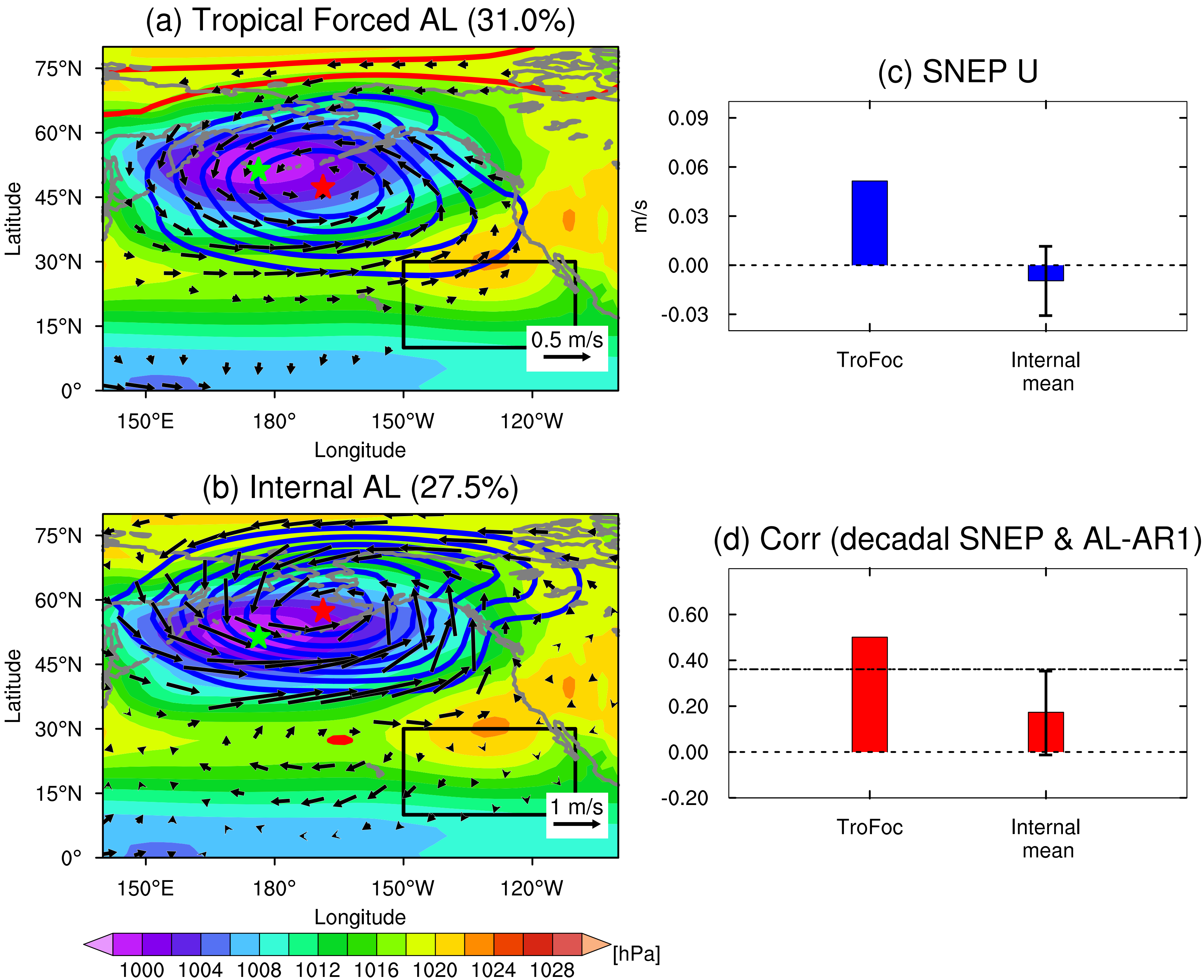

(a) Tropical Forced AL (31.0%)
75°N
60°N
45°N
30°N
15°N
0°
Latitude
150°E
180°
150°W
120°W
Longitude
0.5 m/s
(b) Internal AL (27.5%)
1 m/s
1000
1004
1008
1012
1016
1020
1024
1028
[hPa]
(c) SNEP U
m/s
0.09
0.06
0.03
0.00
-0.03
TroFoc
Internal mean
(d) Corr (decadal SNEP & AL-AR1)
0.60
0.40
0.20
0.00
-0.20